sion indicated that the rate limiting kinetic step is ion-ion recombination [reaction (3)].

The wavelength and time-integrated photon flux for the two bands was measured as a function of Ar pressure. The widths of the two bands were calibrated using the spectrum of the $B(\frac{1}{2}) \rightarrow (X\frac{1}{2})$ at 351 and 352 nm and the spectrum of the $C(\frac{3}{2}) \rightarrow A(\frac{3}{2})$ band at 460 nm obtained from short pulse (Febetron 706) e-beam excitation.[7] The results of these measurements are shown in Fig. 1. As the argon pressure is increased the ratio R of the $C\frac{3}{2} \rightarrow A\frac{3}{2}$ intensity to the $B\frac{1}{2} \rightarrow X\frac{1}{2}$ intensity varies from predominantly $B(\frac{1}{2}) \rightarrow X(\frac{1}{2})$ radiation to predominantly $C(\frac{1}{2}) \rightarrow A(\frac{1}{2})$ radiation. For argon pressures above 1 atm, the ratio approaches the value $R = 3 \pm 1$ in agreement with the value obtained under e-beam (Febetron 706) excitation.[7]

These results demonstrate that the $C\frac{3}{2}$ excited state of XeF is energetically lower than the $B\frac{1}{2}$ state. Furthermore, we can estimate the energy separation by assuming that the levels are in collisional equilibrium at the higher pressures. Then

$$R = \frac{A(C\frac{3}{2})}{A(B\frac{1}{2})} \exp[\Delta E(B\frac{1}{2} - C\frac{3}{2})kT],$$

where $A(C\frac{3}{2})$ and $A(B\frac{1}{2})$ are the Einstein coefficients for the $C\frac{3}{2}$ and $B\frac{1}{2}$ states, respectively. If we assume that the ratio of lifetimes is that calculated by Dunning and Hay[4] $[A(C\frac{3}{2})/A(B\frac{1}{2}) \simeq 1/10]$, and that the asymptotic photon flux ratio $R \simeq 3$ arises from thermal equilibrium established by collisions with the 300°K background

gas, we conclude that $\Delta E(B\frac{1}{2} - C\frac{3}{2}) = 700 \pm 70$ cm^{-1}.

This conclusion suggests that the predominance of uv emission under long-pulse e-beam excitation $(R \sim 0.25)$ arises from effective mixing of the $C\frac{3}{2}$ and $B\frac{1}{2}$ states by the energetic (0.1—0.5 eV) electrons present under those conditions. Electron mixing should also be important under discharge excitation. The presence of this lower longer-lived state in XeF should affect the gain and the overall extraction efficiency of a laser operating on the $B\frac{1}{2}$-$X\frac{1}{2}$ transition.

[1]C. A. Brau and J. J. Ewing, J. Chem. Phys. **63**, 4640 (1975).
[2]D. C. Lorents, D. L. Huestis, M. V. McCusker, H. H. Nakano, and R. M. Hill, J. Chem. Phys. (to be published).
[3]M. Krauss, J. Chem. Phys. **67**, 1712 (1977).
[4]T. H. Dunning Jr. and P. J. Hay, J. Chem. Phys. (to be published).
[5]J. Tellinghuisen, P. Tellinghuisen, G. C. Tisone, J. M. Hoffman, and A. K. Hays (unpublished); P. C. Tellinghuisen, J. Tellinghuisen, J. A. Coxon, J. E. Velazco, and D. W. Setser (unpublished).
[6]See Ref. 5 and references cited therein.
[7]D. L. Huestis *et al.*, SRI International Report No. MP 78-07, 1978 (unpublished).
[8]D. J. Eckstrom and K. Y. Tang (private communication).
[9]D. Kligler, D. Pritchard, W. K. Bischel, and C. K. Rhodes, J. Appl. Phys. **49**, 2219 (1978).
[10]R. Burnham and N. Djeu, Appl. Phys. Lett. **29**, 707 (1976).

Observation of amplified phase-conjugate reflection and optical parametric oscillation by degenerate four-wave mixing in a transparent medium[a]

David M. Pepper,[b] Dan Fekete,[c] and Amnon Yariv

California Institute of Technology, Pasadena, California 91125
(Received 10 February 1978; accepted for publication 19 April 1978)

We report on the observation of amplified reflection and optical parametric oscillation via degenerate four-wave mixing in a nonresonant medium. The process is mediated through the third-order nonlinear susceptibility in a transparent liquid medium, CS$_2$. A collinear mixing geometry is utilized to obtain long interaction lengths and polarization discrimination is used to separate the pump and signal fields.

We report on the observation of amplified reflection and optical parametric oscillation using degenerate four-wave mixing in a transparent medium. The generation of a conjugate "time-reversed" field by nonlinear mixing techniques has been recently proposed[1] and observed.[2] Conjugate fields have also been generated by stimulated Brillouin scattering[3-5] and stimulated Raman scattering.[6] The special case of degenerate four-wave mixing to provide a time-reversed replica of a

given optical field has also been discussed theoretically[7-9] and recently observed.[9,10] This four-wave process offers the advantage of obtaining the conjugate field for any general wave front without the limitations imposed by phase-matching requirements. Further, this interaction has been shown theoretically[8,9] to be capable of generating an amplified complex conjugate (time-reversed) version of a given input field and also oscillation.

The experimental arrangement is shown in Fig. 1. Stripped of details, which will be discussed below, it consists of a CS$_2$ cell which is pumped simultaneously by laser beams A_1 and A_2 of the same frequency ω po-
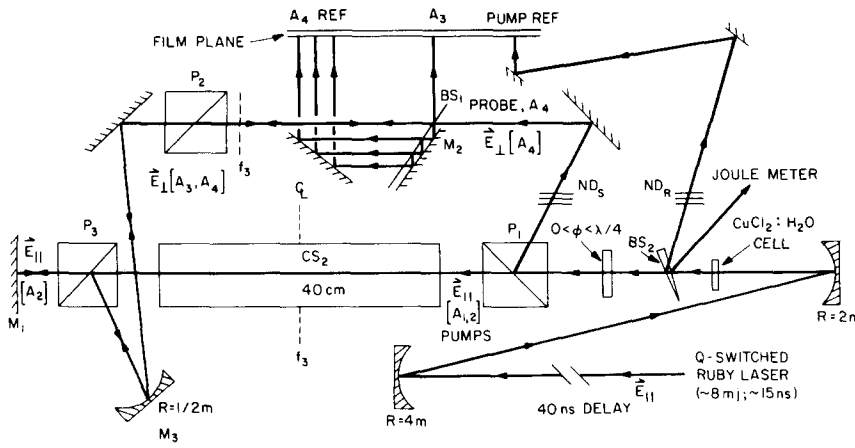
FIG. 1. Experimental apparatus for measurement of the nonlinear reflection coefficient (all mirrors are totally reflecting).

larized in the plane of the figure (parallel, π polarization) and which travel in opposition to each other. Simultaneously, an orthogonally polarized (s) probe beam A_4 at ω is introduced from the left and travels in a direction parallel to that of A_2.

The experiment consists of (1) measuring the intensity of the reflected beam A_3 with polarization parallel to that of A_4 (i.e., orthogonal s polarization) as a function of the pumping intensity ($\sim A_1 A_2$), (2) demonstrate oscillation, i.e., finite outputs at A_3 and A_4 with no corresponding inputs, and (3) to establish that A_3 is the phase conjugate of A_4.

The nonlinear coupling between the various wave components is described by[11]

$$P_y^{\omega_3 = \omega_1 + \omega_2 - \omega_4} = \chi_{yxxy}^{(3)} A_{1x}^{\omega_1 = \omega} A_{2x}^{\omega_2 = \omega} A_{4y}^{*(-\omega_1 = -\omega)}. \tag{1}$$

It has been shown in Ref. 8 that the induced polarization (1) results in an amplification of an input wave A_4 and in a reflected phase conjugate wave A_3 described by

$$A_4(L) = \frac{A_4(0)}{\cos(|\kappa|L)}; \quad A_3(0) = A_4^*(0)[-(i\kappa^*/|\kappa|)\tan(|\kappa|L)], \tag{2}$$

where $\kappa^* = (2\pi\omega/nc)\chi_{NL}^{(3)} A_1 A_2$. Hence the input field A_4 is seen to experience amplification, with the concomitant generation of a conjugate (time-reversed) field propagating in the reverse direction. The reflected field $A_3(0)$ exceeds the input field $A_4(0)$ for $|\kappa|L > \frac{1}{4}\pi$. When $|\kappa|L = \frac{1}{2}\pi$, $A_3(0)$ and $A_4(L)$ are finite even when $A_4(0) = 0$ (i.e., no input). This corresponds to oscillation.

The addition of a mirror along an arbitrary axis was shown in Ref. 8 to reduce the oscillation condition from $|\kappa|L = \frac{1}{2}\pi$ to

$$|\kappa|L = \tan^{-1}(1/|r|), \tag{3}$$

where r is the amplitude reflectivity of the mirror. In the case of perfect mirror, $|r| = 1$, the threshold is $|\kappa|L = \frac{1}{4}\pi$, corresponding to a threshold pumping smaller by a factor of 2 compared to the case of no mirror.

The employment of a collinear geometry for both the signal (A_3, A_4) and pump (A_1, A_2) waves enabled us to use

very long interaction paths and thus realize high gains and even oscillation. This collinear geometry entails the use of $\chi_{yxxy}^{(3)}$ in the nonlinear coupling. Since for CS_2,[12] $\chi_{yxxy}^{(3)}/\chi_{xxxx} \simeq 0.706$, the small loss in coupling is easily tolerable.

The nonlinear reflection coefficient was measured using the experimental arrangement illustrated in Fig. 1. The pump source was a passively Q-switched ruby laser, operating in both a single longitudinal and transverse mode.[13] The laser output was monitored for each shot to ensure single-mode and single-pulse operation. A typical output pulse energy was 7–13 mJ with a duration of 15 ns. The typical intensity spot size was determined[5] to be 2.2 mm in diameter.

The output beam was reflected by a 2:1 spherical mirror collimator and folded to yield an optical path delay of 40 ns before entering the interaction region. Thus, return signals were prevented from reaching the laser throughout the duration of the pulse. A 1-cm-thick cell containing varying concentrations of $CuCl_2$ in H_2O was used to attenuate the laser beam for various input energies.[13] The beam passed next through a calcite Glan laser prism (P_1), and then into the CS_2 medium, which was contained in a 40-cm-long 2-cm-diameter glass cell. Mirror M_1 retroreflected the pump beam giving rise to a counterpropagating component A_2. The cell was tilted off axis to prevent Fresnel reflections from interfering with measured fields. Prism P_1 served a dual function: it passed the pump beam (A_1), "π" polarized into the interaction medium, and in addition coupled an "s" polarized probe pulse (A_4) of order 10^{-3} that of the pump energy (energy determined by the orientation of a retardation plate, ϕ). This probe was then beam split and passed through a calibrated beam-splitter—mirror system (BS_1, M_2) providing a sequence of reflected beams, each being reduced in intensity by a factor of 2, which were incident upon the film plane. For comparison, a Fresnel reflected (via BS_2) pump beam was also recorded. Both of these beams were attenuated through neutral density stacks (ND_S and ND_R) prior to impinging on the film plane, which employed type 47, 3000 ASA high-speed oscilloscope film. The laser energy was monitored by a calibrated Fresnel reflection (off BS_2) using a Gen-Tec model No. ED-100 pyroelectric detector and model No. PRJ-D digital readout.
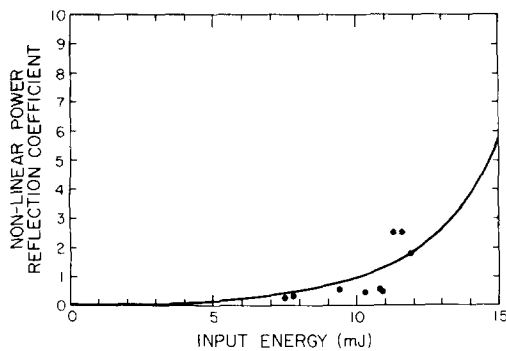
FIG. 2. Plot of nonlinear power relfection coefficient versus pump energy (in mJ). Data (●); least-squares fit to R = $\tan^2(\alpha\epsilon_p)$ (solid line).

The forward-going probe beam, A_4, propagated through prism P_2, oriented to pass s-polarized fields (thus serving to eliminate any scattered or Fresnel reflected π-polarized fields from interfering with the measurement) and was then coupled into the CS_2 cell through a spherical mirror M_3 and another Glan laser prism P_3 (oriented similar to that of P_1) between the cell and M_1. Thus, prisms P_1 and P_3 constrained the probe beam to interact only in the CS_2 cell. The purpose of M_3 was to focus and confine the probe to propagate within the pump beam volume.

The phase conjugate nature of the reflected wave, i.e., $A_3(0) \propto A_4^*(0)$, was established through the use of the mirror M_3 (see Fig. 1). This mirror focuses the collimated input probe beam A_4 on the midplane f_3. A phase conjugate reflection A_3, being a "time-reversed" replica of the input wave A_4, should emerge from the CS_2 cell with virtual emanation from the focal spot at f_3 and thus be collimated. That this was the case was established using the beam spot photographs (taken by reflecting A_3 off BS_1) in the film plane.

The nonlinear nature of the reflected wave was also

established through its temporal (pulse shortening), spatial (well-defined spot size), and frequency (via Fabry-Perot spectra) characteristics. The laser energy was measured before and after the CS_2 cell to ensure that the pump intensity was below that for the onset of stimulated Brillouin scattering. Also, the laser spot size was measured on either side of the cell to verify that self-focusing was not taking place.

The presence of mirror M_3 ensures that only reflected phase conjugated rad'ˑtion is collimated in the film plane. The presence of unwanted s-polarized radiation due to residual birefringence in the optical components, to imperfect extinction in the polarizers, and to ellipse rotation in CS_2[14] gave rise to a divergent output and did not affect the measurement of the reflection coefficient materially.

Figure 2 shows the measured reflection coefficient as a function of the pumping pulse energy, ϵ_p. We note that for energies exceeding 11 mJ the reflection coefficient exceeds unity. Also plotted in Fig. 2 is a least-squares fit of the function

$$R = \tan^2(\alpha\epsilon_p) \tag{4}$$

which is in the form predicted by Eq. (2). The value of α thus determined is employed, using Eq. (2), to calculate the value of $\chi_{yxxy}^{(3)}$ of CS_2. The result is

$$\chi_{yxxy}^{(3)} = (1.64^{+0.14}_{-0.20}) \times 10^{-12} \text{ esu} \tag{5}$$

compared with a generally accepted value[12] of $\chi^{(3)} \sim 1.8 \times 10^{-12}$ esu. This check serves to reassure us that the observed reflection is due to the four-wave mixing process described by Eq. (2).

Self-oscillation was observed using the apparatus shown in Fig. 3. The difference between the two experimental geometries is twofold: first, prism P_1 is used to couple out any oscillation ("s" polarized) signal, while passing the pump beams. Second, the absence of prism P_3 now allows the totally reflecting flat mirror M_1 to serve a dual function: (1) it retro-reflects the pump beam (A_1), thus providing for its counterpropagating component (A_2) and (2) M_1 serves as
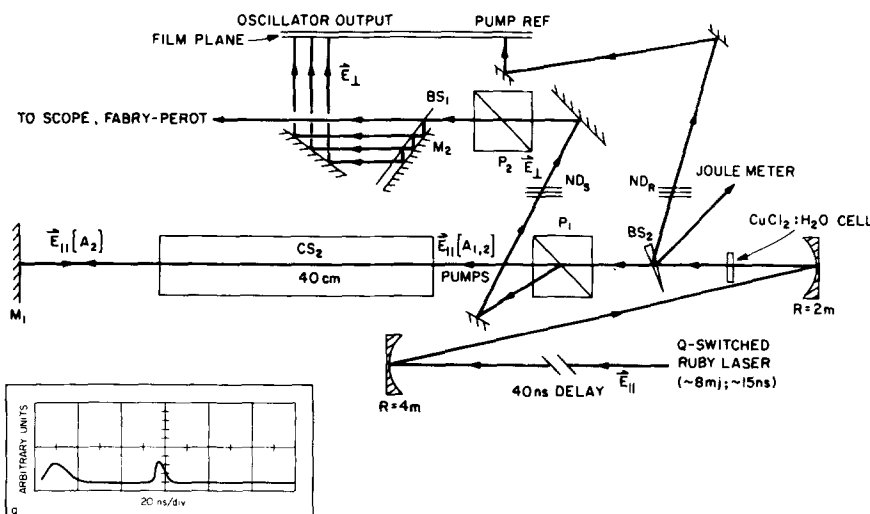

FIG. 3. Experimental apparatus for viewing oscillation. Inset: oscillator output characteristics: Time evolution of pump (left) and oscillator (right) outputs.

a reflector for the orthogonally polarized oscillation field. As discussed above, this reduced the oscillation threshold by a factor of 2.

At pumping intensities exceeding 8.8 MW/cm^2 and with no input field [$A_4(0) = 0$] an intense *oscillation* pulse with orthogonal (s) polarization resulted. The oscillation pulse energy was approximately 1% of the pump energy. It was noted that the spot size of the oscillation beam was smaller than that of the input pump beam. This is due to the fact that the coupling constant κ in Eq. (2) is proportional to the product of two beams, A_1 and A_2, each with a Gaussian intensity profile.

A typical set of temporal pulse shapes is shown in Fig. 3(a). The first pulse is the ruby pump laser output, while the second pulse (properly delayed and of arbitrary amplitude) is the output due to the oscillation. The nonlinearity of the interaction is also evident from this datum. Since the nonlinear gain requires the temporal overlap of the pump beams, the evolution of the gain in the time domain is essentially the temporal convolution of the two Gaussian pulses. This results in a nonlinear gain with a sharper and shorter Gaussian temporal characteristic. Fabry-Perot spectra of these signals verified the degenerate frequency nature of the oscillator output. Finally, the threshold nature of the oscillator output was verified by the nonlinear increase of its output as a function of input pump energy.

In conclusion, we have demonstrated that, in addition to phase conjugation, the process of four-wave mixing can result in amplification and oscillation, in accordance with theoretical predictions.[8] Polarization discrimination was used to separate pump and signal beams. The temporal, spatial, and frequency characteristics of the observed signals were shown to be consistent with those expected from such a nonlinear interaction.

The use of a collinear geometry affords the possibility of performing real-time holographic operations[15] and (time-reversed) image compensation at efficiencies large enough as to be of practical interest than previously observed.

[1]A. Yariv, Appl. Phys. Lett. **28**, 99 (1976).
[2]P. V. Avizonis, F. A. Hopf, W. D. Bomberger, S. F. Jacobs, A. Tomita, and K. H. Womack, Appl. Phys. Lett. **31**, 435 (1977).
[3]B. Y. Zel'dovich, V. I. Popovichev, V. V. Ragul'skii, and F. S. Faisullov, Sov. Phys.-JETP Lett. **15**, 109 (1972).
[4]O. Y. Nosach, V. I. Popovichev, V. V. Ragul'skii, and F. S. Faisullov, Sov. Phys.-JETP Lett. **16**, 435 (1972).
[5]V. Wang and C. R. Giuliano, Opt. Lett. **2**, 4 (1978).
[6]B. Y. Zel'dovich, N. A. Mel'nikov, N. F. Pilipetskii, and V. V. Ragul'skii, Sov. Phys.-JETP Lett. **25**, 36 (1977).
[7]R. W. Hellwarth, J. Opt. Soc. Am. **67**, 1 (1977).
[8]A. Yariv and D. M. Pepper, Opt. Lett. **1**, 16 (1977).
[9]D. M. Bloom and G. C. Bjorklund, Appl. Phys. Lett. **31**, 592 (1977).
[10]S. M. Jensen and R. W. Hellwarth, Appl. Phys. Lett. **32**, 166 (1978).
[11]P. D. Maker and R. W. Terhune, Phys. Rev. **137**, A801 (1965).
[12]R. W. Hellwarth, *Progress in Quantum Electronics* (Pergamon, New York, 1977), Vol. 5.
[13]B. E. Newnam and L. G. DeShazer, in *Damage in Laser Materials*, NBS Special Publication No. 356 (U. S. GPO, Washington, D. C., 1971), p. 113; L. G. DeShazer and J. H. Parks, *ibid.*, p. 124.
[14]See, for example, R. W. Hellwarth, A. Owyoung, and Nicholas George, Phys. Rev. A **4**, 2342 (1971).
[15]Amnon Yariv, Opt. Commun. **25**, 23 (1978).

Room-temperature operation of lattice-matched InP/Ga$_{0.47}$In$_{0.53}$As/InP double-heterostructure lasers grown by MBE

B. I. Miller, J. H. McFee, R. J. Martin, and P. K. Tien

Bell Telephone Laboratories, Holmdel, New Jersey 07733

Molecular beam epitaxial (MBE) growth of InP/Ga$_{0.47}$In$_{0.53}$As/InP double heterostructures has resulted in pulsed room-temperature lasing at 1.65 μm. Thresholds as low as 3.2 kA/cm^2 for a 0.6-μm-thick layer has been achieved. These results were achieved by "premixing" the Ga and In together in a common source oven and precisely monitoring the Ga/In flux ratio during the growth of the Ga$_{0.47}$In$_{0.53}$As layer. Cd diffusion from a vapor source allowed us to p dope the top InP layer in the as-grown MBE wafer.

We report here the room-temperature operation of lattice-matched InP/Ga$_{0.47}$In$_{0.53}$As/InP double-heterostructure lasers grown by molecular beam epitaxy (MBE). Thresholds as low as 3.2 kA/cm^2 for an 0.6-μm active layer have been achieved at a wavelength of 1.65 μm. This result was made possible by the following innovations: (1) "Premixing" the Ga and In together in a common source, (2) precise lattice matching by real-time monitoring of the Ga/In flux ratio, and (3) the ability to p dope the as-grown MBE-grown InP top cladding layer by a Cd postdiffusion.

Earlier results at these long wavelengths have given